This is the Pre-Published Version.
P. Sun, S. Lin, X. Huang (2020) *Ignition of Thin Fuel by Thermoplastic Drips: An Experimental Study for the Dripping Ignition Theory,* **Fire Safety Journal,** https://doi.org/10.1016/j.firesaf.2020.103006

Ignition of Thin Fuel by Thermoplastic Drips: An Experimental Study for the Dripping Ignition Theory

Peiyi Sun, Shaorun Lin, Xinyan Huang*

Research Centre for Fire Engineering, Department of Building Services Engineering, Hong Kong Polytechnic University, Kowloon, Hong Kong xy.huang@polyu.edu.hk

Abstract: Ignition by dripping flame is widely observed in wire fires and façade fires, but little research has quantified its fire hazard. This work studies the ignition of thin papers (0.07 – 0.32 mm) by burning polyethylene drips with four sizes (2.6 - 6.2 mg) and dripping frequencies (0.8 – 1.8 Hz). The probability of dripping ignition as a function of key dripping parameters is quantified to determine the ignition limits. As the paper thickness increases, more drips and longer time are required for ignition, similar to the classical pilot ignition of thin fuels. The attached flame acts as the piloted source; heating effects from hot drips and dripping flame are comparable; and ignition occurs to the paper rather than landed drips. Moreover, the dripping-ignition capability is controlled by the dripping mass rate, which is the product of the drip mass and the dripping frequency. For the dripping mass rate of about 4.5 mg/s, the equivalent heat flux is 15 ± 3 kW/m^2. The dripping-ignition time is inversely proportional to the mass of drip and the square of the dripping frequency, different from the piloted ignition under irradiation. This work provides important information to quantify the fire hazard of dripping and explores the ignition mechanism in dripping fire.

Keywords: polyethylene drip; drip size; ignition limit; thin paper; dripping mass rate

Nomenclature

Symbols

A	area (mm^2)
c	specific heat (kJ/kg-K)
d	diameter (mm)
D	drip diameter (mm)
f	frequency (Hz)
g	gravity acceleration (m/s^2)
h	convection coefficient (W/m^2-K)
H	enthalpy (MJ/kg)
ΔH_c	heat of reaction (MJ/kg)
k	thermal conductivity (W/m-K)
l	length (m)
m	mass (g)
$\dot{m}$	mass rate (mg/s)
M_{dr}	mass of one drip (mg)
n	experiment number (-)
N	number of drips (-)
$\dot{q}''$	heat flux (kW/m^2)
$\dot{q}''_{loss}$	heat loss (kW/m^2)
S	dripping parameter (kg/ s^2)
t	time (s)
T	temperature (℃)
V	volume (cm^3)
Y	mass fraction (-)

Greeks

α	radiation absorptance (-)
γ	surface tension (N/m)
ε	emissivity
σ	Stefan–Boltzmann constant (W·m^{-2}·K^{-4})
δ	thickness (mm)
ρ	density (kg/m^3)
η	heating efficiency (%)

Subscripts

a	ambient
c	charring
dr	dripping
f	flame
F	gaseous fuel
g	gas
ig	ignition
L	landing
m	melting
max	maximum
min	minimum
p	paper
PE	polyethylene
tot	total

1. Introduction

The dripping phenomenon in fire occurs when the weight of melting fuel overcomes its surface tension to produce drips or dripping flows [1]. As dripping is often produced from a burning material and is hot enough to catch fire easily [2], the flame often attaches to drip, i.e., the dripping fire. Dripping is widely observed in the electrical wire fire [3–5] and building façade fire [6], as shown in Fig. 1. It is because the wire insulation [4,5], thermal insulation layer of the building façade [2], and billboard are often made by thermoplastics that are easy to melt, such as the polyethylene (PE), polyethylene chloride (PVC), polypropylene (PP) and expanded polystyrene (EPS) [7,8]. Once a fire occurs, drips from burning plastic fuel could ignite other materials to promote the fire spread, therefore, increasing the fire hazards [2]. For example, numerous dripping fires detached from the burning molten PE of aluminum composite material (ACM) panel were observed in the 2017 London Grenfell Tower fire, which could also contribute to the rapid fire-spread process [6].

Figure 1. The dripping phenomenon and the resulted ignition process in (a) the electrical wire fire, and (b) a façade fire in China, and (c) Grenfell Tower fire in London [9].

In the literature, most studies on flaming ignition focus on the piloted-ignition and auto-ignition behaviors of solid materials, which are well-reviewed in [10–12]. However, very little research has studied the fire phenomenon of dripping and its capability of igniting other fuels, mainly because of the complex fire process. One major complexity is the interaction between two fuels, (1) the non-ignited target fuel, and (2) the ignited drips. In other words, the observed dripping ignition could either be the ignition of target fuel or the sustained flame on landed drips. In addition, phase-change processes between gas, liquid and solid fuels, such as the melting and pyrolysis, and the flame attachment to fast falling drip are also complex [1].

Most dripping-related literature focuses on the generation of drips from fire. For example, Wang *et al*. [8] studied the dripping behavior in the UL94 standard test{Formatting Citation} and quantified the size of drip from different thermoplastics. Xie *et al.* [2] found at least 400 ℃ was required for molten PP, PE, and PS to flow easily, which is higher than their pyrolysis temperature, and autoignition was observed when the high-temperature drip was in contact with air. He *et al*. [3] found that overload currents played an important role in promoting the fire spread over the wire, and the dripping frequency increased with the current. Kobayashi *et al*. [4] revealed that the dripping flow of molten polymer would increase the downward fire spread. Fang *et al.* [14] found that the propensity of dripping from the wire fire varied with the ambient pressure and oxygen concentration. Several numerical models have been proposed to simulate the generation of dripping in wire [15,16] and the burning thermoplastics in the UL94 test [17]. Recently, Jiang *et al.* [18] studied the melting and dripping effect on ignition of thermally thick PE and PP slabs, and

established a heat transfer model to explain the ignition process. In our previous work [1], the ignitability of PE drip was found to depend on whether the drip can carry a flame or not. If a PE drip was larger than 2.3 mm, it can carry a flame during the free fall for at least 2.6 m (i.e., one floor) and ignite an ultra-thin tissue paper of 0.02-mm thickness. However, the ignition capability of dripping is still unknown for many common thin and thick fuels. Moreover, it is not clear whether the process of dripping ignition follows the classical ignition theories, so there is a big knowledge gap.

In this work, we focus on the dripping ignition of thin papers with different thicknesses. Well-controlled experiments are designed and conducted to explore the ignition capability of continual PE drips with flame. The size and number of drips are controlled to find the limiting ignition conditions, and then, the mechanism of dripping ignition is explored.

2. Experiment methods

2.1. Apparatus and dripping generation

The experimental setup was upgraded from the previous work [1], and the schematic diagram is shown in Fig. 2(a). Drips were produced by burning a horizontal PE tube. A metal tube was inserted into the PE tube, and then fixed to the sample holder. Once the flame spread over the PE tube became steady-state, the continual generation of drips also became steady-state with a relatively stable frequency.

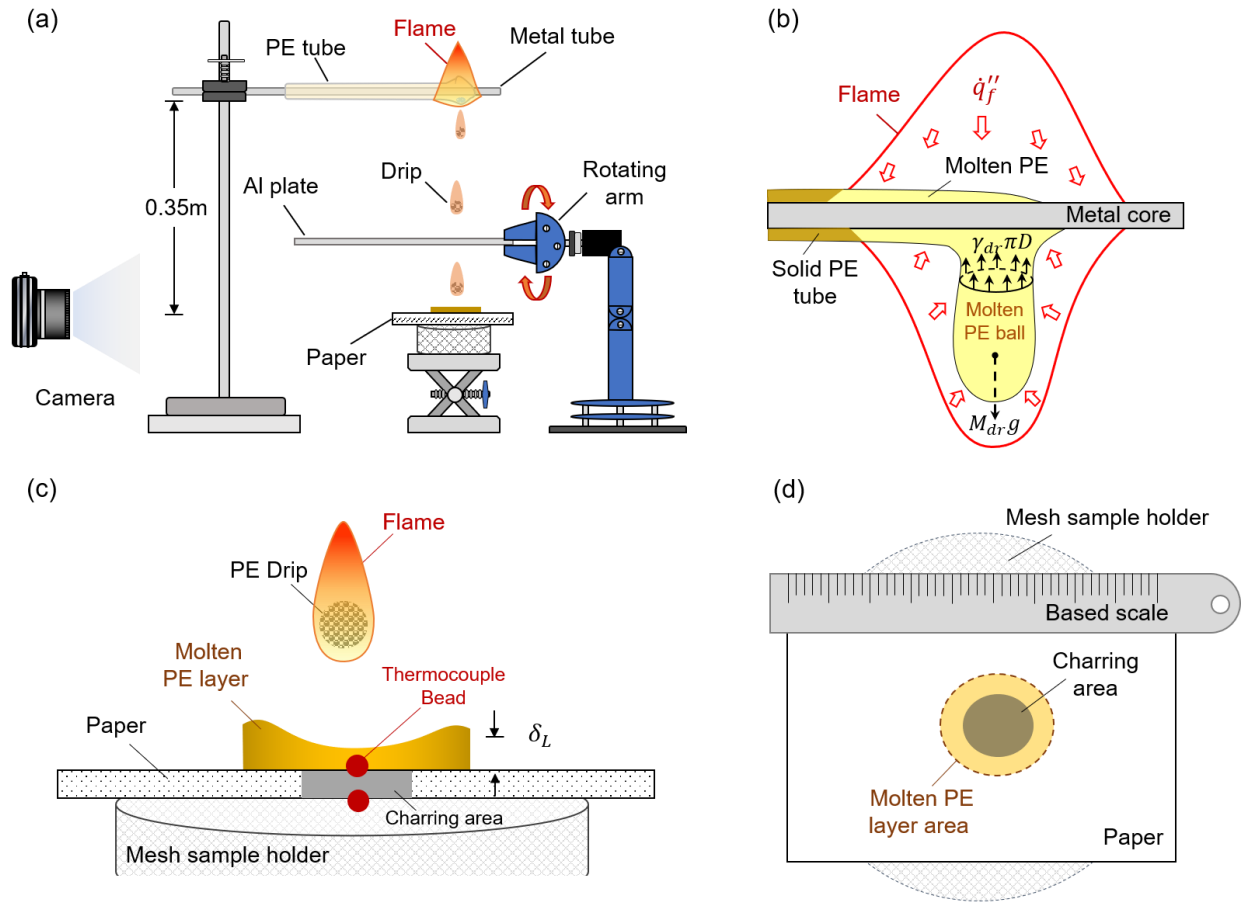

Figure 2. Schematic diagrams of (a) the experiment apparatus, (b) the formation of molten PE ball before dripping, (c) the accumulation of dripping layers on the paper surface, and (d) the top view for critical ignition area and charring area on the paper sample.

In order to control the size and frequency of drips, PE tubes, and metal tubes with different wall thicknesses were used. As illustrated in Fig. 2(b), the burning PE was heated by the flame while cooled by the metal tube, and the molten PE would form a ball with a diameter of (D) hang on the tube before dripping. The gravity of molten PE ($M_{dr}g$) is the driven force of dripping, which increases with the size of the PE ball [4]. While the surface tension (γ_{dr}) is the resistance of dripping, which increases significantly with the decreasing temperature [19]. The drip will be detached if its gravity force overcomes its surface tension as

$$M_{dr}g = \rho_{dr}\left(\frac{\pi}{6}D^3\right)g \geq \gamma_{dr}(\pi D) \quad (1)$$

If the surface tension of molten PE becomes larger, only larger drips can overcome gravity and get detached. Therefore, larger drips could be produced from the metal tube with a larger wall thickness (i.e., a larger cooling effect). In addition, the burning speed of the thicker wire is slower because of the larger fuel load and stronger cooling effect, which results in the lower dripping frequency (f_{dr}). In other words, the dripping mass is inversely correlated with the dripping frequency.

2.2. Materials

In this experiment, drips of four different sizes (Types A-D, 2.6–6.2 mg) were produced, as listed in Table 1. The mass of drip (M_{dr}) was measured by a precision balance (±0.1 mg), and its random uncertainty was less than 10% for multiple repeating tests. The dripping frequency (f_{dr} = 0.8–1.8 Hz) was measured from the video, where smaller drips had a higher frequency. The smallest drip (2.6 mg) sometimes showed an irregular dripping frequency and formed a continuous dripping flow, and such a special condition was not considered. Video imaging process also revealed that during the fall, the shape was not a perfect sphere but an ellipsoid. Also, the drip was porous, because there was a strong bubbling process as well as many small bubbles inside the drip, as illustrated in Fig. 2(c). For simplicity, the equivalent diameter of the spherical drip (D_{dr}) can be estimated with the bulk density of the porous PE drip (ρ_{dr} = 640 kg/m^3), as listed in Table 1.

Table 1. Characteristics of drips tested in experiments, where the uncertainty is less than 10%.

Drip Type	**A**	**B**	**C**	**D**
Mass of drip, M_{dr} (mg)	2.6	3.3	4.6	6.2
Dripping frequency, f_{dr} (Hz)	1.8	1.4	1.0	0.8
Drip diameter, D_{dr} (mm)	2.0	2.1	2.4	2.6
Landing diameter, d_L (mm)	6.7	7.7	9.6	11.3
Landing thickness, δ_L (mm)	0.12	0.11	0.10	0.10

Once the drip lands on the surface of tested fuel, the PE drip would self-compress into a thin cylindrical layer of PE with the landing diameter (d_L) and thickness (δ_L), as listed in Table 1. Despite a small amount of molten PE was splashed into tiny drips that flied away, the majority mass would stay on the paper. As drips continued to land on the paper, a semi-circular molten PE layer was formed, and the paper started to char. The molten PE layer area (A_m) and the charring area (A_c) on paper were measured through photos from the top view, as illustrated in Fig. 2(d). Both areas increased with the number of drips until ignition.

Three different printer papers (Type I-III) as the characteristic thin fuel were tested. Their surface densities were 75 g/m^2, 140 g/m^2 and 300 g/m^2, and their equivalent thicknesses (δ_p = 0.07 ~ 0.32 mm) were proportional to their surface densities, as listed in Table 2. Note that these paper samples were much thicker and less porous than previously tested ultra-thin tissue paper (δ_p = 0.02 mm) [1], thus, they could not be ignited by a single small drip. The size of all paper samples was fixed to 10 cm × 7 cm (i.e., 1/8 of

the A4 paper). The tested paper was placed horizontally on the top of a tubular mesh, so that the bottom of the paper was exposed to air.

Table 2. Characteristics of paper tested in experiments where the density of paper is 930 kg/m^3.

Paper Type	I	II	III
Surface density (g/m^2)	75	140	300
Thickness, δ_p (mm)	0.07	0.15	0.32
Radiation absorptance, α_p (%)	58 ± 2	69 ± 5	72 ± 5

To quantify the flammability of these papers, their piloted ignition delay time was also measured using the cone calorimeter (FTT iCone Plus) under different irradiations. During the test, metal frames were used to fix the paper sample and prevent the curling in the edge. Considering the thin paper could not absorb all radiation energy, part of the radiation would transmit through the paper. The radiation reached the top surface of the paper and transmitted through the paper was measured by the radiometer. Then, the absorptance of cone radiation (α_p) for each paper was calculated, as listed in Table 2, and as expected, it increased with the thickness of the paper.

2.3. Procedures and measurements

In prior to the dripping ignition test, the PE tube was first ignited by a lighter. The flame was allowed to develop and spread along the PE tube where drips were generated in a stable and periodical manner. only drips within a stable dripping frequency were selected and tested. The distance between burning PE tube (source fuel) and the paper sample (target fuel) was fixed to be 0.35 m. Such a small fall height ensured that the flame would always attach to the drip during the fall [1]. The ignition intensity was controlled by the number of drips (N). To better control the number of drips landing on the paper, a control system including the alumina (Al) plate, robot arm, and a PC was assembled. The robot arm was controlled by the PC to rotate the Al plate to either prevent or allow drips to land on the paper, as illustrated in Fig. 2(a).

To access the heat transfer process during the dripping ignition, temperatures on both the top and the bottom surfaces of paper were measured by two pairs of thermal couples, as seen in Fig. 2(c). The thermocouples (TCs) were made by welding the 0.03-mm thick chromel and alumel wires, so their bead diameter was less than 0.1 mm. The temperature data were collected by a data logger every 0.1 s, which was much shorter than the interval of two drips (about 1 s).

The testing process was recorded by a camera (Sony RX10) with a shooting speed of up to 960 fps. Because the size and frequency of drips could not be perfectly controlled, and the ignition process was complex, a large experimental uncertainty was expected. Thus, to estimate the ignition probability, more than 100 tests were repeated for each combination of drip and paper types. In total, more than 2,000 dripping-ignition tests were conducted in this study.

3. Results and discussions

3.1. Dripping ignition phenomena

Figure 3 shows a typical dripping ignition process of the Type I paper (δ_p = 0.07 mm) after landing different numbers of drips (Type B: M_{dr} = 3.3 mg, f_{dr} = 1.4 Hz). For all drips, they carry a flame before landing. After five drips (Fig. 3a and Video 1), the region of paper, covered by the hot molten PE layer, was gradually charred, but the flaming ignition did not occur. In another test, the ignition was successful after six drips (Fig. 3b and Video 2), and the flame could burn out the paper. Throughout the experiment, only flaming ignition occurred, smoldering ignition of paper was never observed.

To understand the role of dripping flame, the high-speed camera was used to capture the detailed landing process of the drip and the dripping flame above the paper top surface. As shown in Fig. 4, the residence time of flame on the paper surface was less than 0.1 s, which was shorter than the interval of about 1 s between drips. For the first a few drips (Fig. 4a), the dripping flame tended to form a small pool flame above the landed molten PE layer, but it was quickly quenched by the cool paper. During the impact, multiple tiny flamelets flied away with splashing tiny PE droplets. For the last a few drips before ignition (Fig. 4b), the dripping flame also ignited the flammable mixture above the landed drips. Such a flaming process is like a small explosion, and the following propagation of blue flame above the paper could also be observed. This strong flash is also expected to help drips heat and ignite the paper until a stable flame is sustained on paper. Therefore, the dripping flame not only acts as the piloted source, but its heating effect on paper is also quite important (discussed more in Section 3.3).

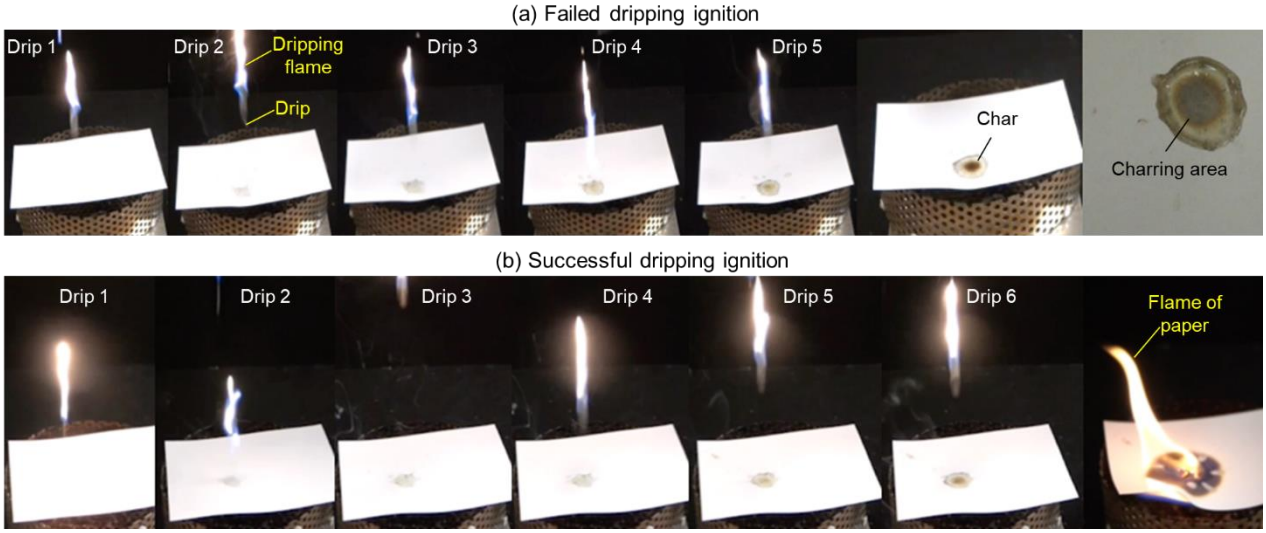

Figure 3. Snapshots of typical dripping ignition process of a Type I paper (0.07 mm) with Drip B (3.3 mg, 1.4 Hz), (a) failed ignition after 5 drips, and (b) successful ignition after 6 drips. More details can be viewed from Videos 1 and 2 in the Supplemental Material.

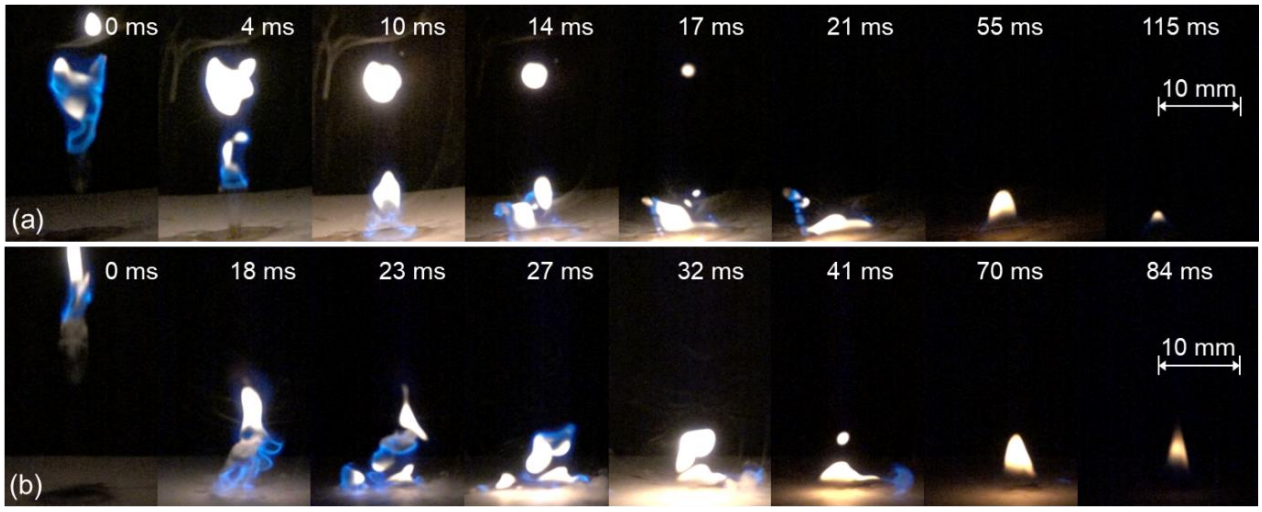

Figure 4. Snapshots of the landing process of the drip and the dripping flame, (a) early stage with weak flame, and (b) a strong flash near the ignition of paper. More details can be viewed from Videos 3 and 4.

3.2. Probability and limiting conditions of dripping ignition

In this work, a successful dripping ignition of thin paper is defined if a stable flame can be sustained to burnout the paper. The ignition probability, correlating the critical number and mass of drips and the density of the paper, is measured through the statistical analysis of many repeating experiments. Referring to past studies on the hot-particle ignition [20,21], the ignition probability (P_{ig}) is defined as the ratio of the number of successful ignitions (n) to the number of repetition (n_{tot}), as

$$P_{ig} = \frac{n_{ig}}{n_{tot}} \times 100\% \tag{2}$$

The ignition probability for three thicknesses of paper (I-III) and four sizes of drips (A-D) is quantified as a function of the number of drips (N) in Fig. 5 and the total mass of drips (M_{ig}) in Fig. 6. Because of the complex dripping process, the varying range of ignition probability increases, as the number of drips and the thickness of paper increases. Here, we define P_{ig} = 50% as the dripping ignition limit that is a function of the mass of drip (M_{dr}), number of drips (N), the total mass of drips (M_{ig}), and the paper thickness (δ_p), as shown in dashed lines and summarized in Figs. 5(d) and 6(d).

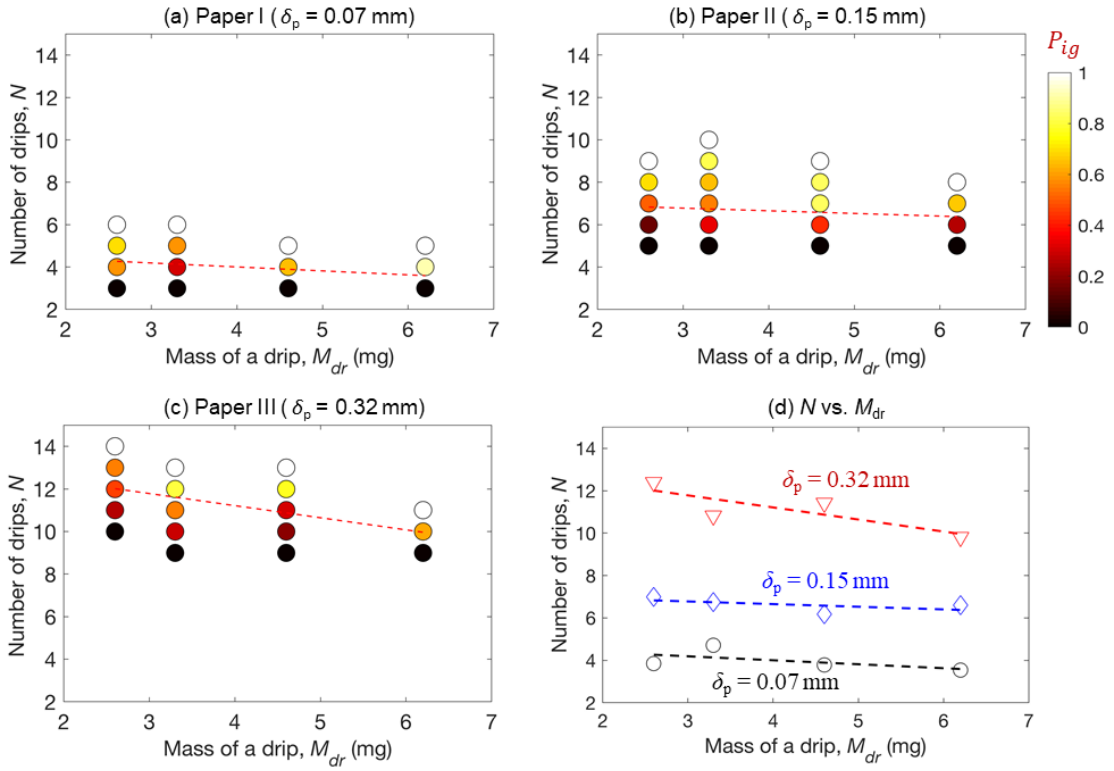

Figure 5. Dripping ignition limit as a function of number drips (N) and the mass of a drip (M_{dr}) for (a) Paper Type I (0.07 mm), (b) Paper Type II (0.15 mm), and (c) Paper Type III (0.32 mm), where the ignition probability (P_{ig}) is scaled by the color bar, and P_{ig} = 50% is the critical ignition condition.

Figures 5 and 6 show that as the paper thickness increases, both the required number of drips and total mass of drips for ignition are increased. Specifically, the thinnest Type I Paper needs about 4 drips to ignite; Type II Paper needs about 7 drips; and the thickest Type III Paper needs 11 drips, where the number of drips is almost proportional to the thickness of the paper. For a thicker paper, its thermal inertia is greater [12], so that greater thermal energy is required to heat the paper up to its critical ignition condition. This

trend demonstrates that the observed ignition phenomenon is the ignition of paper, rather than the self-sustaining process of the dripping flame on the landed drips. Moreover, such a dripping-ignition process of paper also satisfies the classical piloted ignition theory for the thermally-thin fuel, that is, the required ignition energy or the difficulty of ignition increases with the fuel thickness. The dripping flame is the pilot source, without which flame ignition will not occur. Moreover, both the dripping flame and the hot drip are heat sources.

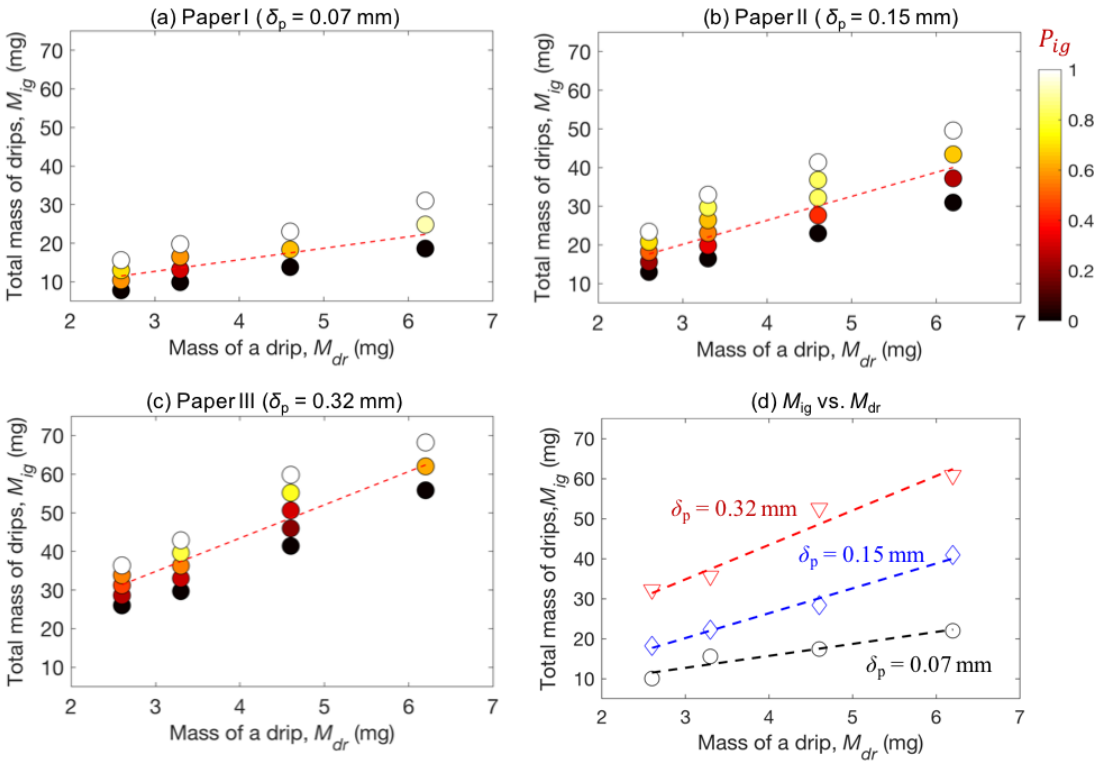

Figure 6. Dripping ignition limit as a function of total mass of drips ($M_{ig} = N{\cdot}M_{dr}$) and the mass of a drip (M_{dr}) for (a) Paper Type I (0.07 mm), (b) Paper Type II (0.15 mm), and (c) Paper Type III (0.32 mm), where the ignition probability (P_{ig}) is scaled by the color bar, and P_{ig} = 50% is the critical ignition condition.

More interestingly, Fig. 5 shows that the required minimum number of drips (N) for ignition is essentially insensitive to (or only slightly decreases with) the mass of the drip (M_{dr}) within the current test range of 2.6-6.2 mg. As a result, the required total mass of drips (NM_{dr}) will increase almost linearly with the mass of a single drip in Fig. 6. This result is unexpected, because a larger mass of drip means a greater amount of thermal energy to heat and ignite the paper. Therefore, the dripping ignition cannot be simply explained by the conventional approach of ignition energy [22], because the heating from drips to paper is discrete, different from the conventionally continuous radiant and convective heating [23].

To understand such a trend, the dripping frequency (f_{dr}) has to be considered, which increases with the mass of drip in this experiment (see Table 1 and Fig. 7). Then, we can define the **dripping mass rate** ($\dot{m}_{dr}$) as the average mass of drips per unit time

$$\dot{m}_{dr} = M_{dr} f_{dr} \tag{3}$$

which is the key parameter to quantify the ignition limit and fire hazard of dripping. Figure 7 shows that $\dot{m}_{dr}$ is almost a constant (4.5 ± 0.5 mg/s) for different drip sizes, because the smaller drip has a higher

dripping frequency. Such a constant dripping mass rate for different drip sizes leads to the constant minimum number of drips in Fig. 5, which also contributes to a near-uniform dripping heat flux for different drips (discussed in Section 3.3). Based on the definition in Eq. (3), increasing either the mass of drip or the dripping frequency can equally increase the dripping mass rate, as well as the dripping fire hazard.

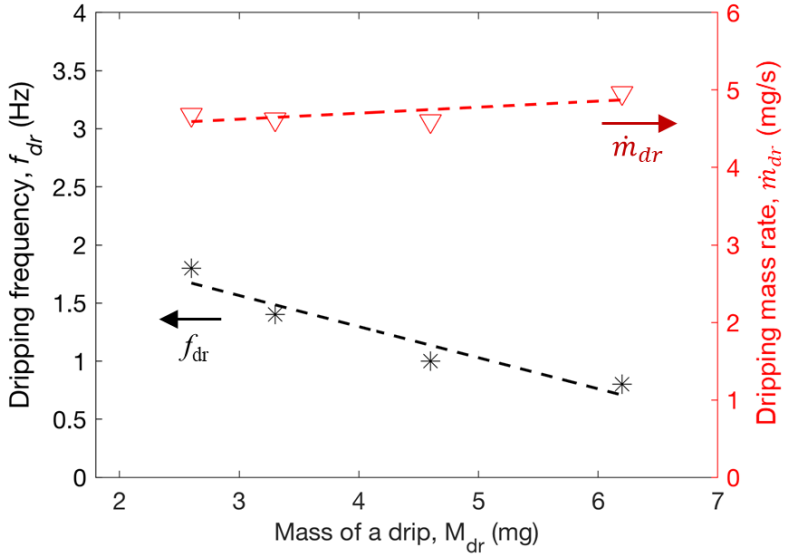

Figure 7. Dripping frequency (f_{dr}) and dripping mass rate ($\dot{m}_{dr}$) versus the single drip mass (M_{dr}).

3.3. Ignition areas and heat flux of dripping

As illustrated in Fig. 2(c-d), after the landing of drips, a molten PE layer will form above the paper. The area of the molten layer (A_m) slowly increases with the number of drips until a maximum of about 3 cm^2, where the molten PE in the edge cools down and solidifies. Note that this molten layer does not have a perfectly cylindrical shape but a bowl shape. The central thickness is smaller than the edge thickness because of the impact of drips. Therefore, the central region of paper is the most heated area, where a charring area (A_c) will form gradually during dripping, and the PE layer becomes more transparent as the temperature increases.

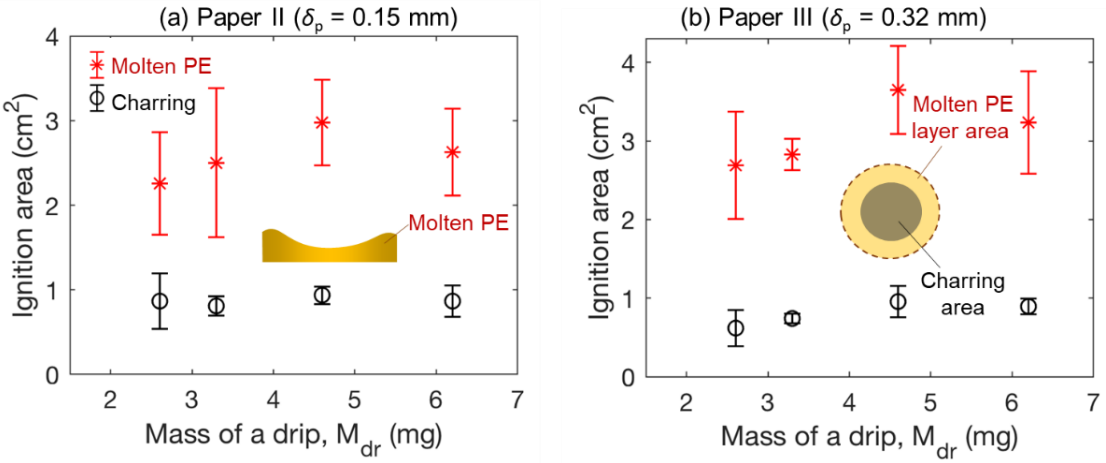

Figure 8. The measured molten PE layer area (A_m) and charring area (A_c) on paper right before ignition, (a) Type II paper (δ_p = 0.15 mm) and (b) Type III paper (δ_p = 0.32 mm).

Figure 8 shows the measured molten PE layer area (A_m) and charring area (A_c) on paper for two paper types right before ignition. In general, the critical area of molten PE layer approaches its maximum, so it does not vary significantly for different drip sizes, especially when the number of drips gets larger for thicker papers. Moreover, the charring area is essentially a constant ($A_c \approx 1$ cm^2) before ignition, which is insensitive to any parameters. These similarities suggested that the dripping heating area on the paper are similar for different drip size, probably because they have a similar dripping mass rate, as shown in Fig. 7.

Figure 9 shows the thermocouple temperature measurement of the paper top and back surfaces during the dripping-ignition process. It can be seen that there is a sharp temperature increase on the paper top surface right after the landing of drip and flame for about 0.1 s (see Fig. 4). Afterward, the flame extinguishes so that the top-surface temperature decreases before the arrival of the next drip. Due to the relatively high dripping frequency, the top surface temperature increases gradually drip by drip. More importantly, in all experiments, the ignition occurs when the top-surface temperature of the paper exceeds about 400 ºC, which can be defined as the ignition temperature.

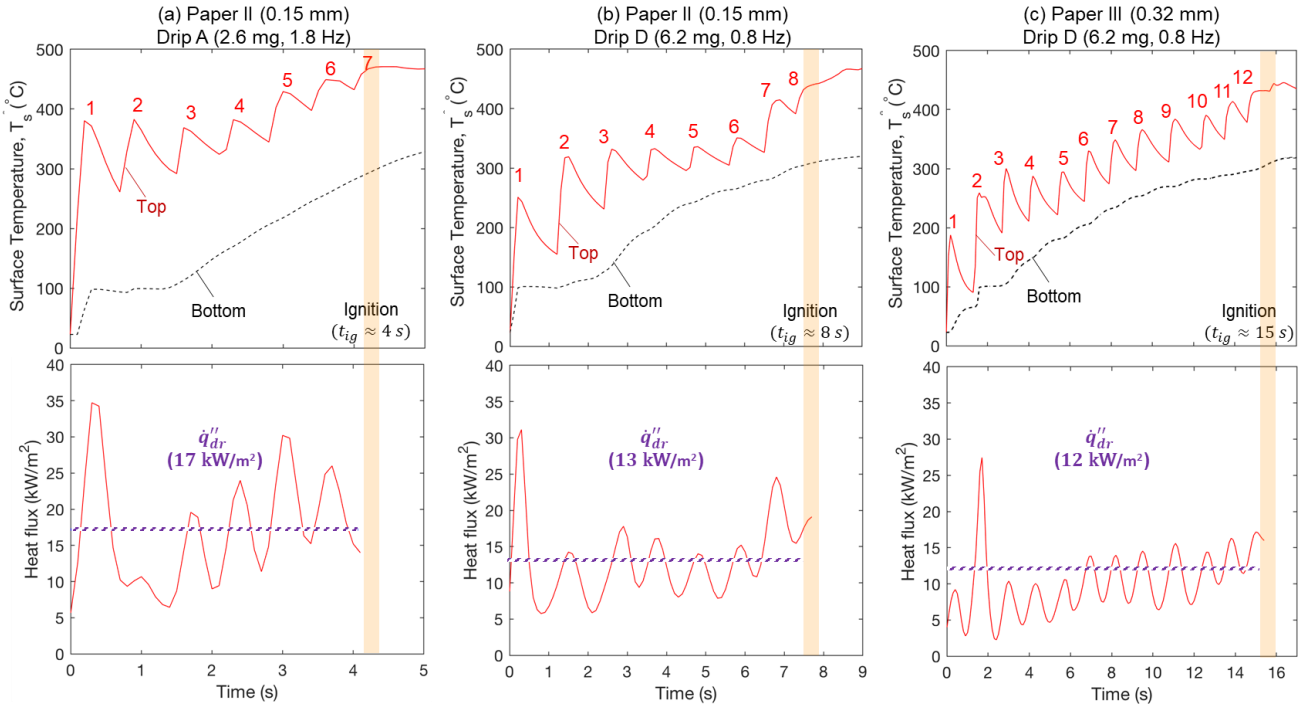

Figure 9. the evolution of paper surface temperatures and the calculated equivalent heat flux during the dripping ignition process, (a) Type II paper (δ_p = 0.15 mm) with Drip A, (b) Type II paper (δ_p = 0.15 mm) with Drip D, and (c) Type III paper (δ_p = 0.32 mm) with Drip D.

On the other hand, the back surface temperature of the paper is weakly affected by the discrete landing process of drips while showing a monotonic increase. Moreover, the temperature measurements suggest that there should be a minimum dripping frequency ($f_{dr,min}$), below which the top surface of paper cannot be heated above the ignition temperature of 400 ºC. With the same paper type (δ_p = 0.15 mm) and dripping mass rate ($\dot{m}_{dr} = 4.5$ mg/s), comparison between Fig. 9(a) and (b) shows that as the dripping frequency increases, the ignition delay time (t_{ig}) decreases. With the same drip mass (M_{dr} = 6.2 mg) and dripping frequency (f_{dr} = 0.8 Hz), comparison between Fig. 9(b) and (c) shows that as the thickness of paper increases, the overall heating rate of paper decreases, and the ignition time increases.

Based on the temperature evolution, the equivalent dripping heat flux ($\dot{q}''_{dr}$) on the thermally thin fuel can be estimated by using a lumped heat transfer model [10] as

$$\dot{q}''_{dr} = \rho_p c_p \delta_p \frac{dT_p}{dt} + \dot{q}''_{loss} \tag{4a}$$

where $\rho_p = 930$ kg/m^3, $c_p = 1.34$ kJ/kg-K [24], δ_p, and T_p are the density, specific heat, thickness, and the average temperature of paper below the molten PE layer, respectively. The heating rate of paper (dT_p/dt) can be acquired from the thermocouple measurement. Because the top surface of the paper is covered by the hotter molten PE and the short-term dripping flame, only the transient heat loss on the bottom surface of the paper ($\dot{q}''_{loss}$) should be considered as

$$\dot{q}''_{loss} = h(T_p - T_a) + \varepsilon_p \sigma (T_p^4 - T_a^4) \tag{5}$$

where $h \approx 10$ W/m^2-K is the convective coefficient [25]; $T_a = 295$ K is the room temperature; $\varepsilon_p = 0.95$ is the emissivity of paper; and $\sigma = 5.67 \times 10^{-8}$ W·m^{-2}·K^{-4} is the Stefan–Boltzmann constant.

Figure 9 also shows the calculated equivalent dripping heat flux ($\dot{q}''_{dr}$) based on the temperature evolution. Like the temperature measurement, the dripping heat flux also shows a large and frequent fluctuation concerning the arrival of each drip. As expected, the heat flux of the first drip is the largest, because the paper is the only fuel to heat up. While for later drips, they also need to heat the thin layer of molten PE above the paper, leading to a smaller fluctuation. Eventually, the equivalent dripping heat flux approaches to a constant, $\dot{q}''_{dr} = 15 \pm 3$ kW/m^2, for the majority date with different dripping and paper conditions, as summarized in Fig. 10(a).

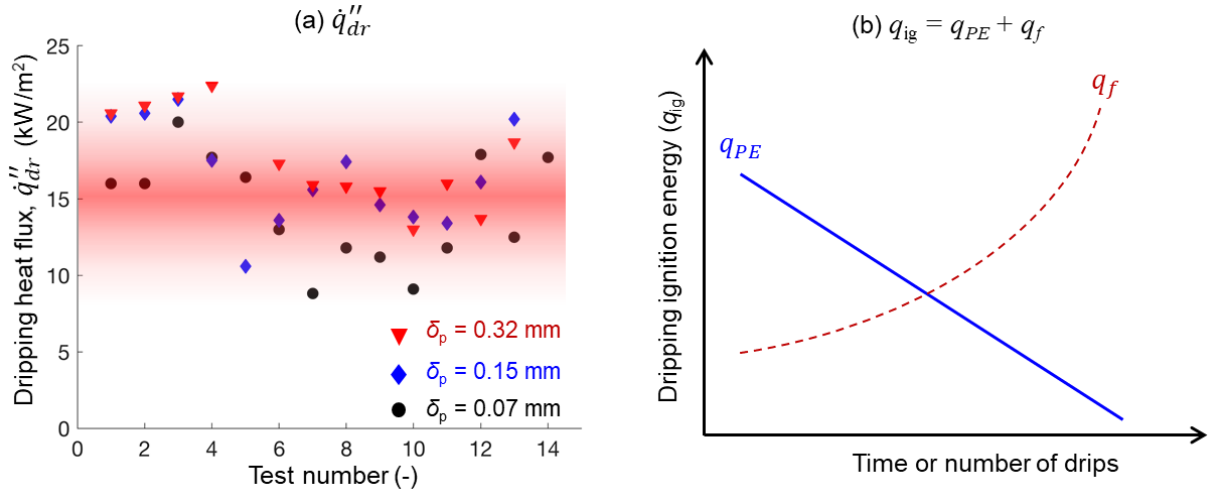

Figure 10. (a) Measured equivalent dripping heat flux ($\dot{q}''_{dr}$), and (b) the ignition energy of the hot drip (q_{PE}) and the dripping flame (q_f).

Both the hot drip and dripping flame are heat sources; thus, it is important to compare their relative importance and estimate the total ignition energy of the drip plus flame (q_{ig}). For each PE drip, its effective ignition energy increases with drip mass (M_{dr}) while decreasing with the paper temperature (T_p)

$$q_{PE} = M_{dr} H_{PE} = M_{dr} c_{PE} (T_{PE} - T_p) \approx 0.4 \text{ - } 2.7 \text{ J} \tag{6}$$

where $c_{PE} = 1.55$ kJ/kg-K is the specific heat of PE [26]; $T_{PE} \approx 400$℃ is the pyrolysis temperature of PE [2,27]; and the paper temperature T_p is lower than its pyrolysis temperature of 350 ℃ [24]. For the

Type C drip of M_{dr} = 4.6 mg, the ignition energy of a hot drip decreases with time from 2.7 J to 0.4 J, as the paper temperature increases from 22 ℃ to 350 ℃.

On the other hand, the dripping flame includes both the flame attached to the drip and the flame ignited above the paper (Fig. 4). The ignition energy of dripping flame (q_f) can be estimated as

$$q_f = Y_F \rho_g V_g \Delta H_F \approx 1.3 \text{ - } 3.8 \text{ J} \tag{7}$$

where $Y_F \approx 6.3\%$ uses the stoichiometric mass fraction of ethylene to represent that of PE pyrolysis gases; $\rho_g \approx 0.5$ kg/m^3 is the density of gas mixture; $\Delta H_F \approx 40$ MJ/kg is the heat of combustion of PE [10]; and V_g is the volume of the flammable mixture, which can be estimated by the flame size from the high-speed imaging. As the number of landed drips increases, the volume of the flammable mixture becomes larger, so that the flame becomes stronger, as shown in Fig. 4. As V_g increases from 1 cm^3 to 3 cm^3, the ignition energy of dripping flame increases with time from 1.3 J to 3.8 J.

Therefore, the ignition energies of the hot drip and dripping flame are *comparable*. Moreover, as the number of drips or time increases, the heating effect of hot drip decreases while that of dripping flame increases, as summarized in Fig. 10(b). As a result, the overall ignition energy of a 5-mg drip with flame is about $q_{ig} = q_{PE} + q_f \approx 4$ J throughout the dripping process. Then, the total ignition energy flux of dripping can be estimated as

$$\dot{q}''_{tot} = \frac{(q_{PE} + q_f) f_{dr}}{\bar{A}} = \frac{\dot{m}_{dr} H_{PE} + q_f f_{dr}}{\bar{A}} \approx 20 \text{ kW/m}^2 \tag{8}$$

where $\bar{A} = (A_m + A_c)/2 \approx 2$ cm^2 is the effective heating area; and $f_{dr} \approx 1$ Hz. Therefore, the equivalent dripping heat flux ($\dot{q}''_{dr}$) can be estimated as

$$\dot{q}''_{dr} = \eta \dot{q}''_{tot} = \frac{\eta}{\bar{A}} \left(\dot{m}_{dr} H_{PE} + q_f f_{dr} \right) = \frac{\eta}{\bar{A}} \left(M_{dr} H_{PE} + q_f \right) f_{dr} \tag{4b}$$

where the heating efficiency (η) is calculated to be about 70% from Fig. 9 and Eq. (4a), which is reasonable, because part of the energy is dissipated to the environment. As expected, the dripping heat flux increases with the dripping mass rate ($\dot{m}_{dr} = M_{dr} f_{dr}$), that is, with both the drip mass and dripping frequency. As the ignition energy of dripping flame (q_f) also implicitly depends on the drip mass, the influence of dripping frequency and the drip mass on equivalent dripping heat flux also be comparable.

3.4. Dripping-ignition time and theory

To quantify the dripping ignition behaviors, the dripping-ignition time ($t_{ig,dr}$) and equivalent dripping heat flux ($\dot{q}''_{dr}$) for three paper types are plotted in Fig. 11. For a better comparison, the ignition time measured from the cone-calorimeter experiments is plotted as well. The ignition delay time increases with the thickness of paper (δ_p) and decreases with the cone radiation ($\dot{q}''_c$), which satisfies the classical thermally thin theory as

$$t_{ig,c} \approx \frac{\rho_p c_p \delta_p \left(T_{ig} - T_\infty \right)}{\alpha_p \dot{q}''_c - \dot{q}''_{loss}} \tag{9}$$

where α_p is the irradiation absorbance of paper which increases with the thickness (see Table 2). Note that during the cone ignition, both top and bottom surfaces of the paper are cooled by the environment. In contrast, during the dripping ignition, only the bottom surface of the paper is cooled, while the top surface is covered and heated by the hot PE layer.

The comparison shows that the ignition time of dripping increases with the thickness of paper, because the dripping-ignition process is similar to the piloted ignition process, as discussed in Section 3.2. However, compared to the piloted ignition time under the cone irradiation, the dripping-ignition time is much shorter, and the possible ignition region is well below the ignition curve, as shown in Fig. 11. It is because (1) the dripping ignition process reduces environmental heat loss from the top surface of the paper, and (2) the equivalent dripping heat flux is transient, which can reach large heat flux value periodically (see Fig. 9).

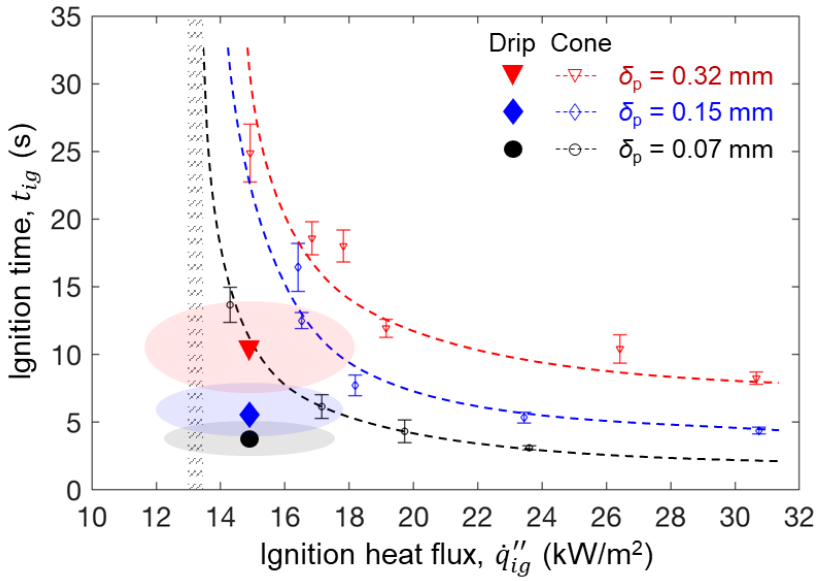

Figure 11. Ignition time of dripping and cone-calorimeter experiments for three paper thicknesses, where the shadow region indicates the uncertainty of dripping-ignition time and heat flux.

Considering the similarity between the dripping ignition and the piloted ignition under the cone calorimeter for fuel, the dripping ignition time ($t_{ig,dr}$) should be similar to Eq. (9) as

$$t_{ig,dr} \propto \frac{\delta}{\dot{q}''_{dr}} \propto \frac{\delta}{\dot{m}_{dr}} = \frac{\delta}{M_{dr} f_{dr}} \tag{10a}$$

which increases with the fuel thickness and decreases with the ignition heat flux. Based on Eq. (4), the dripping ignition heat flux ($\dot{q}''_{dr}$) increases with the dripping mass rate ($\dot{m}_{dr} = M_{dr} f_{dr}$). Note that despite the dripping mass rate is almost the same (4.5 mg/s) for different drip sizes (Fig. 7), their ignition time is different (e.g. Fig. 9a-b), that is, shorter for the larger dripping frequency.

On the other hand, the dimensionless analysis can correlate the ignition time with the dripping frequency as

$$t_{ig,dr} \propto \frac{1}{f_{dr}} \tag{10b}$$

That is, with an increasing dripping frequency, the dripping-ignition time decreases, as verified by the experimental data in Fig. 12(a). Such a trend is unique for dripping ignition, because of the dripping frequency is a time-related parameter.

Therefore, combining Eq. (10a) and (10b), the dripping-ignition time should satisfy

$$t_{ig,dr} \propto \frac{\delta}{\dot{m}_{dr} f_{dr}} = \frac{\delta}{M_{dr} f_{dr}^2} = \frac{\delta}{S} = \frac{\text{Resistance of thin fuel}}{\text{Driven force of dripping}} \tag{10c}$$

where we can introduce a parameter (S) to quantify the driven force of dripping ignition as

$$S = M_{dr} f_{dr}^2 \tag{11}$$

The experimental data show an excellent linear trend (R^2 = 0.96) in Fig. 12(b), so they verify the proposed correlation for the dripping-ignition time in Eq. (10c). Therefore, the ignition delay time is inversely proportional to the mass of drip and the square of the dripping frequency, which is very different from the classical piloted ignition theory in Eq. (9). In other words, dripping frequency has a greater influence on the ignition time than the drip mass.

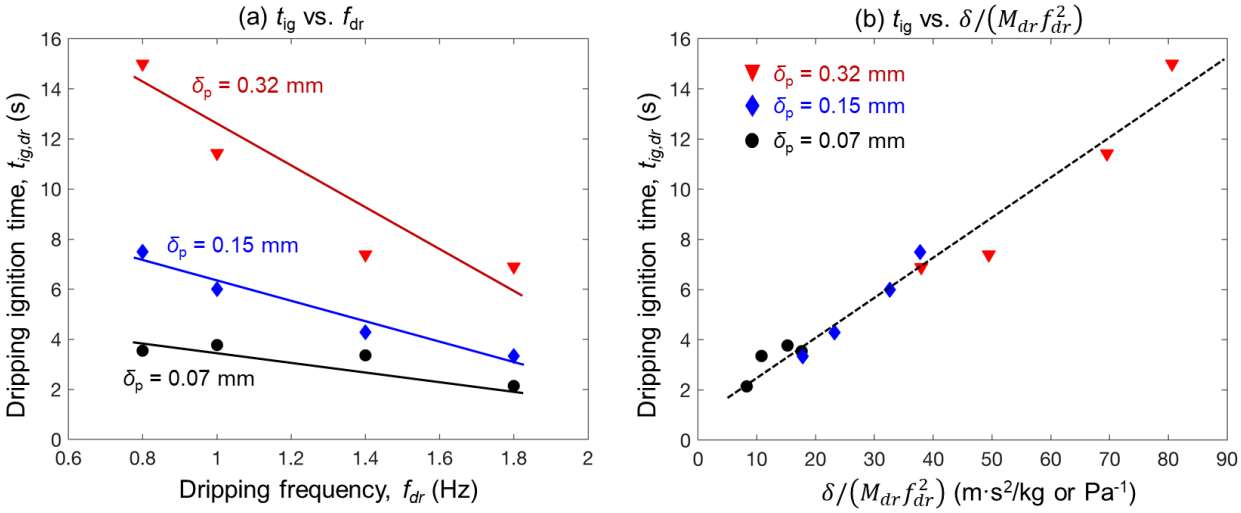

Figure 12. The dripping-ignition time as a function of (a) dripping frequency in Eq. (10a), and (b)

3.5. Extrapolation of dripping ignition limits

In this experimental study, the tested mass of PE drips ranges from 2.6 mg to 6.2 mg, and the dripping frequency ranges from 0.8 Hz to 1.8 Hz. Both the drip size and the dripping frequency are limited not only by the experimental apparatus but also by the thermophysical properties of PE. As found in experiments, it is not possible to produce a PE drip larger than 7 mg, larger than which the internal PE will not be fully molten. For drips smaller than 2.6 mg, the burning mass loss during the free fall becomes important, and the dripping flame may be extinguished [1]. On the other hand, for the dripping frequency larger than 2 Hz, drips may form a continuous dripping flow surrounded by a long flame. While for dripping frequency smaller than 0.3 Hz, the paper won't be ignited.

It is expected that there is a minimum dripping mass rate ($\dot{m}_{min}$) and a minimum dripping frequency (f_{min}), as hypothesized in Fig. 13. Below such a minimum value, no matter how many drips arrives on the target fuel, flaming ignition would not occur. Such critical values are expected to vary with the type of drip fuels. Moreover, as the mass of a single drip gradually increases, eventually, only one drip is needed to ignite the thin fuel. Then, dripping ignition becomes controlled by the mass of drip, where a critical drip mass of supreme fire hazard (M_{dr}^*) may be found to define the upper limit of the dripping mass rate ($\dot{m}_{max} = M_{dr}^*/\Delta t$). Moreover, these critical values are expected to increase with the thickness of fuel.

Note that for thermally thick fuels, the dripping-ignition behaviors could be much more different, because (1) the observed flaming ignition may be a self-sustainment of the dripping flame, and (2) the thick fuel may not be ignited after the burnout of molten layers. Also, dripping can achieve smoldering ignition of certain fuels, even if there is no flame attached to the drip. As many unknowns remain, more experimental and numerical studies are needed in the future to verify these hypotheses.

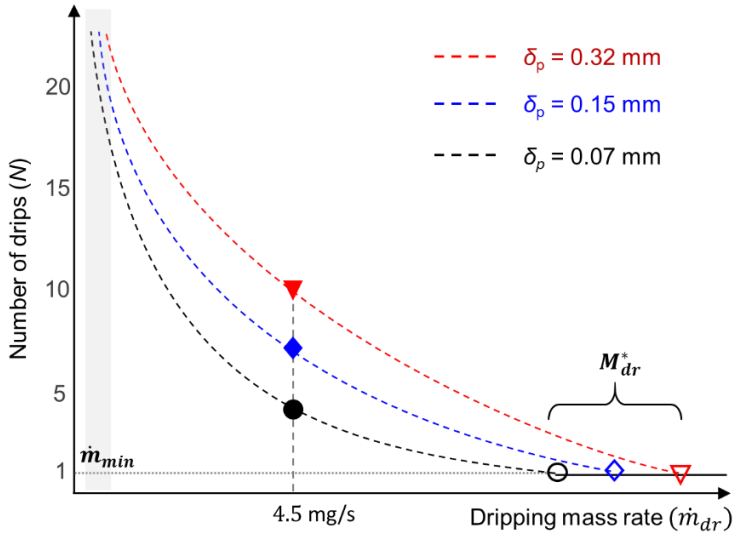

Figure 13. The hypothesized trend of the critical number (N) of drips vs. the dripping mass rate ($\dot{m}_{min}$).

4. Conclusions

In this work, dripping-ignition behaviors are studied by using burning polyethylene drips with four sizes (2.6 - 6.2 mg) and corresponding dripping frequency ranging from 0.8 to 1.8 Hz. Printer papers with three thicknesses (0.07 - 0.32 mm) are chosen as typical thin fuels. The probability of dripping ignition as a function of key dripping parameters is quantified to determine the ignition limits.

Results show that as the paper thickness increases, more drips are required for ignition, indicating the ignition occurs to the paper rather than landed drips. The dripping ignition is similar to the classical pilot ignition of thermally thin fuels, but the controlling parameters are very different. That is, for dripping ignition, the attached flame acts as the piloted source; the heating effects from both hot drips and dripping flame are important; and the total ignition energy of a 5-mg PE drip is about 4 J per drip which is transferred to the targeted fuel drip by drip continually.

Moreover, the capability of dripping ignition is controlled by the dripping mass rate, which is the product of drip mass and dripping frequency. The temperature measurements show that the equivalent dripping heat flux is 15 ± 3 kW/m^2 for the dripping mass rate of about 4.5 mg/s. The dripping-ignition time is inversely proportional to the square of dripping frequency and the mass of drip, different from the piloted ignition under irradiation. Future work will investigate the dripping mass and frequency separately to explore how these two parameters determine the ignition progress. This study provides important information to quantify the fire hazard of dripping and explores the ignition mechanism in the dripping fire. The proposed dripping ignition theory can be further verified and applied to evaluate and classify the ignition capability (fire risks) for different thermoplastic materials.

Acknowledgments

This research is supported by the Hong Kong Polytechnic University (BE04) and National Natural Science Foundation of China (NSFC) No. 51876183.

CRediT author statement

Peiyi Sun: Investigation, Writing - Original Draft, Formal analysis; **Shaorun Lin**: Investigation, Resources; **Xinyan Huang**: Methodology, Conceptualization, Supervision, Writing - Review & Editing.

References

[1] X. Huang, Critical Drip Size and Blue Flame Shedding of Dripping Ignition in Fire, Scientific Reports. 8 (2018) 16528. https://doi.org/10.1038/s41598-018-34620-3.

[2] Q. Xie, R. Tu, N. Wang, X. Ma, X. Jiang, Experimental study on flowing burning behaviors of a pool fire with dripping of melted thermoplastics, Journal of Hazardous Materials. 267 (2014) 48–54. https://doi.org/10.1016/j.jhazmat.2013.12.033.

[3] H. He, Q. Zhang, R. Tu, L. Zhao, J. Liu, Y. Zhang, Molten thermoplastic dripping behavior induced by flame spread over wire insulation under overload currents, Journal of Hazardous Materials. 320 (2016) 628–634. https://doi.org/10.1016/j.jhazmat.2016.07.070.

[4] Y. Kobayashi, X. Huang, S. Nakaya, M. Tsue, C. Fernandez-Pello, Flame spread over horizontal and vertical wires: The role of dripping and core, Fire Safety Journal. 91 (2017) 112–122. https://doi.org/10.1016/j.firesaf.2017.03.047.

[5] X. Huang, Y. Nakamura, A Review of Fundamental Combustion Phenomena in Wire Fires, Fire Technology. 56 (2020) 315–360. https://doi.org/10.1007/s10694-019-00918-5.

[6] S.T. McKenna, N. Jones, G. Peck, K. Dickens, W. Pawelec, S. Oradei, S. Harris, A.A. Stec, T.R. Hull, Fire behaviour of modern façade materials – Understanding the Grenfell Tower fire, Journal of Hazardous Materials. 368 (2019) 115–123. https://doi.org/10.1016/j.jhazmat.2018.12.077.

[7] Y. Wang, J. Zhang, Thermal stabilities of drops of burning thermoplastics under the UL 94 vertical test conditions, Journal of Hazardous Materials. 246–247 (2013) 103–109. https://doi.org/10.1016/j.jhazmat.2012.12.020.

[8] Y. Wang, J. Jow, K. Su, J. Zhang, Dripping behavior of burning polymers under UL94 vertical test conditions, Journal of Fire Sciences. 30 (2012) 477–501. https://doi.org/10.1177/0734904112446125.

[9] I. Groome, What is cladding? The material involved in the Grenfell Tower fire, Metro News. (2017). https://metro.co.uk/2017/06/14/what-is-cladding-the-material-involved-in-the-grenfell-tower-fire-6707949/.

[10] J.G. Quintiere, Fundamental of Fire Phenomena, John Wiley, New York, 2006. https://doi.org/10.1002/0470091150.

[11] A. Atreya, Ignition of fires, Phil. Trans. R. Soc. Lond. A. 356 (1998) 2787–2813. https://doi.org/10.1098/rsta.1998.0298.

[12] D. Drysdale, An Introduction to Fire Dynamics, 3rd ed., John Wiley & Sons, Ltd, Chichester, UK, 2011. https://doi.org/10.1002/9781119975465.

[13] Underwriters Laboratories, Test for Flammability of Plastic Materials for Parts in Devices and Appliances, 1996.

[14] J. Fang, Y. Xue, X. Huang, J. Wang, S. Zhao, X. He, L. Zhao, Dripping and Fire Extinction Limits of Thin Wire: Effect of Pressure and Oxygen, Combustion Science and Technology. (2019). https://doi.org/10.1080/00102202.2019.1658578.

[15] Y. Kim, A. Hossain, Y. Nakamura, Numerical study of melting of a phase change material (PCM) enhanced by deformation of a liquid–gas interface, International Journal of Heat and Mass Transfer. 63 (2013) 101–112. https://doi.org/10.1016/j.ijheatmasstransfer.2013.03.052.

[16] Y. Kim, A. Hossain, Y. Nakamura, Numerical modeling of melting and dripping process of polymeric material subjected to moving heat flux: Prediction of drop time, Proceedings of the Combustion Institute. 35 (2015) 2555–2562. https://doi.org/10.1016/j.proci.2014.05.068.

[17] F. Kempel, B. Schartel, J.M. Marti, K.M. Butler, R. Ross, S.R. Idelsohn, E. Oñate, A. Hofmann, Modelling the vertical UL 94 test: competition and collaboration between melt dripping, gasification and combustion, Fire Mateiral. 39 (2015) 570–584. https://doi.org/10.1002/fam.2257.

[18] Y. Jiang, C. Zhai, L. Shi, X. Liu, J. Gong, Assessment of melting and dripping effect on ignition of vertically discrete polypropylene and polyethylene slabs [J], Journal of Thermal Analysis and Calorimetry. (2020). https://doi.org/10.1007/s10973-020-09575-1.

[19] R.A. Mendelson, Polyethylene Melt Viscosity: Shear Rate-Temperature Superposition, Transactions of the Society of Rheology. 9 (1965) 53–63. https://doi.org/10.1122/1.549006.
[20] S. Wang, X. Huang, H. Chen, N. Liu, G. Rein, Ignition of low-density expandable polystyrene foam by a hot particle, Combustion and Flame. 162 (2015) 4112–4118. https://doi.org/10.1016/j.combustflame.2015.08.017.
[21] J.L. Urban, C.D. Zak, C. Fernandez-Pello, Cellulose spot fire ignition by hot metal particles, Proceedings of the Combustion Institute. 35 (2015) 2707–2714. https://doi.org/10.1016/j.proci.2014.05.081.
[22] I. Vermesi, N. Roenner, P. Pironi, R.M. Hadden, G. Rein, Pyrolysis and ignition of a polymer by transient irradiation, Combustion and Flame. 163 (2016) 31–41. https://doi.org/10.1016/j.combustflame.2015.08.006.
[23] S. Mcallister, M. Finney, Autoignition of wood under combined convective and radiative heating, Proceedings of the Combustion Institute. 36 (2017) 3073–3080. https://doi.org/10.1016/j.proci.2016.06.110.
[24] V. Babrauskas, Ignition Handbook, Fire Science Publishers/Society of Fire Protection Engineers, Issaquah, WA, 2003. https://doi.org/10.1023/B:FIRE.0000026981.83829.a5.
[25] T.L. Bergman, A.S. Lavine, F.P. Incropera, D.P. DeWitt, Fundamentals of heat and mass transfer, 2011, USA: John Wiley & Sons. ISBN. 13 (2015) 470–978.
[26] K. Miyamoto, X. Huang, N. Hashimoto, O. Fujita, C. Fernandez-Pello, Limiting Oxygen Concentration (LOC) of Burning Polyethylene Insulated Wires under External Radiation, Fire Safety Journal. 86 (2016) 32–40. https://doi.org/10.1016/j.firesaf.2016.09.004.
[27] A. Tewarson, Flammability of Polymers, in: Plastics and the Environment, John Wiley & Sons, Ltd, Hoboken, NJ, USA, 2004: pp. 403–489. https://doi.org/10.1002/0471721557.ch11.